

A Note on Unrealistic Gravity induced Plasticity in Cohesionless Unbounded Media under a Drucker-Prager Failure Criterion

Doriam Restrepo *

January 29, 2014

Abstract

The onset of plasticity under self-weight conditions is examined in a homogeneous half-space assuming a cohesionless Drucker-Prager failure criterion. Four alternatives to define the Drucker-Prager cone are explored. It is shown that plasticity under static conditions occurs if the Drucker-Prager failure criterion adopts either the Extension-Cone or the Internal-Cone approach for values of the Poisson's ratio $\nu \leq 0.2$. Adopting the Compromise-Cone approach also renders plastic behavior at rest but for $\nu \leq 0.125$. If the Drucker-Prager model is made to coincide at the outer edges of the Mohr-Coulomb criterion i.e. Compression-Cone approach, plasticity under static conditions still appear, but for a range of ν values that depends on the angle of internal friction ϕ . This study shows that this unconventional initial plastic behavior can be avoided by assuming a Compression-Cone approach in addition with the coefficient of lateral pressure at rest proposed by geotechnical estimates.

Keywords: Material nonlinearity, Drucker-Prager, Half-Space.

1 Introduction

Originally formulated for metals, plasticity theory concepts have been successfully transferred to geotechnical problems in such a way that, today, plasticity for geomaterials as a new field, has reached a very wide scope and significant scientific credibility as a consistent framework in soil behavior prediction.

Plasticity in geomaterials adopts the basic elements of flow plasticity theory, (i) existence of an initial *yield surface* or *yielding criterion*, (ii) evolution of subsequent loading surfaces *hardening rule*, and (iii) the

* Associate Professor. Civil Engineering. Universidad EAFIT. Carrera 49 N 7 Sur - 50. Medellín - Colombia. Tel.: +57 (4) 261 9337; E-mail: drestre6@eafit.edu.co

7 existence of an appropriate *flow rule* (Chen and Mizuno, 1990). The definition of the onset of plasticity is
8 governed by the yielding criterion. Flow rules are usually expressed in accordance with associative or non-
9 associative concepts. In associative rules, the plastic flow potential function shares the same definition as the
10 yield surface function, in non-associative rules on the other hand, the flow rule and yielding functions differ.
11 Although the use of associative flow rules may appear as a simple convenient mathematical device, there are
12 much more profound mathematical reasons for its usage. For instance, it ensures well-posed boundary value
13 problems, uniqueness of the solution and preserves the validity of the so called stability postulates (Drucker,
14 1959).

15 To date, the number of advanced constitutive models that accurately describe the soil rheology at differ-
16 ent strain levels is abundant. Most of these models however, focus on predicting the local nonlinear response
17 by means of increasingly complex expressions based upon a large number of variables that cannot be easily
18 obtained from standard laboratory tests. Moreover, most of these constitutive models base under the as-
19 sumption that numerical integration can be performed in a straightforward manner, even when it has been
20 shown that they are susceptible to numerical failure (Borja and Lee, 1990). Conversely, simple elastoplas-
21 tic constitutive models despite their modest nature, still remain as the prevalent strategies in geotechnical
22 modeling specially by the engineering community. Certainly, the best known yielding model for soils is the
23 Coulomb's failure criterion, an irregular hexagonal pyramid in the principal stress space. Even when the
24 Coulomb criterion is generally simple, and depends on physical parameters readily obtained from conven-
25 tional laboratory results, it gives rise to numerical difficulties regarding the plastic flow at the corners of the
26 yielding surface. Aiming at representing a more appealing model computational-wise Drucker and Prager
27 (1952) presented a smooth function that approximates the Coulomb model as a cone in the principal stress
28 space. In the Drucker-Prager model, the yielding surface is expressed in terms of the first invariant of the
29 stress tensor I_1 , the second invariant of the deviatoric stress tensor J_2 and two material constants α and κ .
30 This allows a straightforward backward-implicit integration scheme for the material update algorithm at the
31 Gauss point level. As a result, the Drucker-Prager failure criterion has been widely used in slope stability
32 problems (e.g., Daddazio et al., 1987; Mizuno and Chen, 1983, 1984; Chen and Mizuno, 1990), and another
33 diverse areas such as off-fault earthquake rupture studies (e.g., Ma and Andrews, 2010; Templeton and Rice,
34 2008; Viesca et al., 2008), and large-scale earthquake ground motion simulation (e.g., Restrepo et al., 2012).

35 Despite the widespread use of Drucker-Prager inelasticity, this paper brings to attention the likelihood
36 of irregular predictions of nonlinear behavior by such a material model. Evidence of unrealistic plasticity

37 is presented by examining a the response of a simple cohesionless half-space subjected merely to gravity
 38 stresses. Since such a domain does not exhibit any geometrical irregularity, nor the in situ stress state
 39 generates irregular stress patterns within the soil mass, the response of any material point should be elastic
 40 irrespective of state variables or material model definitions. Although the study of geometrically unperturbed
 41 half-spaces to gravity forces is not a relevant engineering problem, it is of paramount importance in nonlinear
 42 earthquake ground motion simulation where surficial irregularities are generally disregarded, and is accepted
 43 that prior to the occurrence of the seismic event, the initial gravity induced stress state is elastic. Surprisingly,
 44 my results show that elastic stresses violate the failure criterion for some specific ranges of the Poisson's
 45 ratio. My results show also that linear conditions at rest can be restored if one adopts the coefficient of
 46 lateral pressure traditionally used in geotechnical estimates.

47 **Model Description**

48 Assuming standard linear elastic theory is straightforward to prove that under the action of the self-weight
 49 γ , the principal stress-state at any material point z in a homogeneous half-space is purely compressional and
 50 fully described in terms of the vertical stress component σ_z , the elastic coefficient of lateral pressure at rest
 51 K_o , and the Poisson's ratio ν . Fig. 1.

$$\sigma_z = -\gamma z; \quad K_o = \frac{\nu}{1 - \nu} . \quad (1)$$

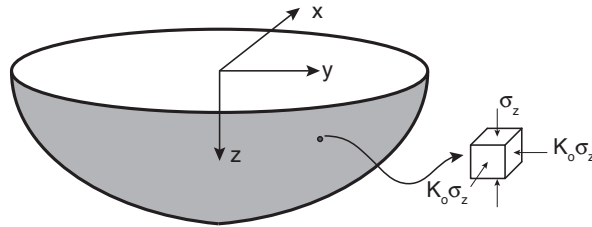


Figure 1: Stress-state in a homogeneous half-space subjected to gravity load.

52 The first invariant of the stress tensor I_1 and the square root of the second invariant of the deviatoric
 53 stress tensor $\sqrt{J_2}$, take the following values for the static condition (superscript *st*)

$$I_1^{st} = (1 + 2K_o) \sigma_z , \quad (2)$$

$$\sqrt{J_2^{st}} = \frac{|\sigma_z|(1 - K_o)}{\sqrt{3}}. \quad (3)$$

54 One of the best known yielding model for soils is the Mohr-Coulomb's failure criterion. Despite its
 55 simplicity, the Mohr-Coulomb model gives rise to numerical difficulties regarding the plastic flow at the
 56 corners of the yielding surface when used in general 3D stress states. Aiming at representing a more appeal-
 57 ing model computational-wise, [Drucker and Prager \(1952\)](#) presented a smooth function that approximates
 58 the Mohr-Coulomb model as a cone in the principal stress space. In this model, the onset of plasticity in a
 59 cohesive-frictional geomaterial with friction angle ϕ and cohesion c , begins if I_1 and $\sqrt{J_2}$ satisfy

$$\sqrt{J_2} + \alpha(\phi)I_1 = k(\phi, c), \quad (4)$$

60 the material variables k and α in Eq. (4) can be characterized depending on the criteria adopted for making
 61 coincide the Drucker-Prager failure criterion with the Mohr-Coulomb model. The Compression-Cone and
 62 the Extension-Cone are obtained if the Drucker-Prager model coincides at the outer and inner apices of the
 63 Mohr-coulomb hexagon respectively ([de Souza Neto et al., 2008](#)). These cones are defined by

64 Compression-Cone

$$\alpha = \frac{2 \sin \phi}{\sqrt{3}(3 - \sin \phi)}, \quad k = \frac{6c \cos \phi}{\sqrt{3}(3 - \sin \phi)}. \quad (5)$$

65 Extension-Cone

$$\alpha = \frac{2 \sin \phi}{\sqrt{3}(3 + \sin \phi)}, \quad k = \frac{6c \cos \phi}{\sqrt{3}(3 + \sin \phi)}. \quad (6)$$

66 Two alternative cones, the so-called Compromise-Cone ([Zienkiewicz and Pande, 1977](#)) located some-
 67 where in between the Compression and the Extension cones, and the Internal-Cone ([Griffiths, 1990](#)) placed
 68 completely inside the hexagonal pyramid are obtained according to:

69 Compromise-Cone

$$\alpha = \frac{2 \sin \phi}{3\sqrt{3}}, \quad k = \frac{6c \cos \phi}{3\sqrt{3}}. \quad (7)$$

70 Internal-Cone

$$\alpha = \frac{\sin \phi}{\sqrt{3}(3 + \sin^2 \phi)}, \quad k = \frac{3c \cos \phi}{\sqrt{3}(3 + \sin^2 \phi)}. \quad (8)$$

71 In the meridional plane ($I_1 - \sqrt{J_2}$ plane), Eq. (4) depicts a straight line with slope $-\alpha$ and intercept k .

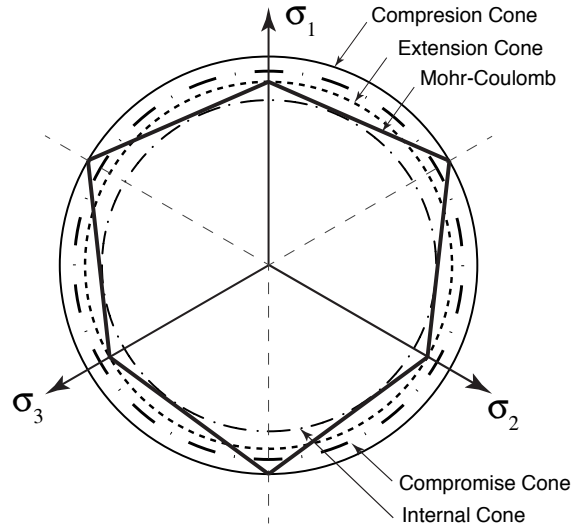


Figure 2: Mohr-Coulomb model and Drucker-Prager approximations in the π plane.

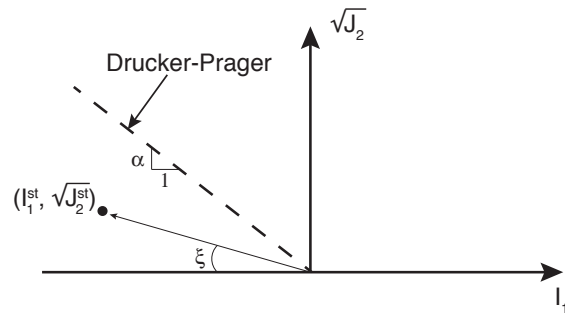


Figure 3: Meridional plane depicting the Drucker-Prager failure criterion for a cohesionless soil, and the initial stress-state under gravity loads.

72 If the geomaterial is *cohesionless*, the k value in Eqs. (5) to (8) vanishes, and the failure criterion becomes
 73 a line that passes through the origin. Fig. 3 depicts the failure criterion for a cohesionless geomaterial,
 74 and the initial stress-state from Eq. (1). In order to ensure elastic behavior under static conditions it is
 75 straightforward to see that the following must hold

$$\tan(\xi) \leq \alpha, \quad (9)$$

76 substituting in Eq. (9) the I_1^{st} and $\sqrt{J_2^{st}}$ values from Eqs. (2) and (3) yields

$$\frac{(1 - K_o)}{\sqrt{3}(1 + 2K_o)} \leq \alpha. \quad (10)$$

77 It becomes clear from Eq. (10) that four different expressions relating K_o and ϕ will be obtained de-
 78 pending on the α value chosen:

79 Compression-Cone

$$\sin \phi \geq \frac{(1 - K_o)}{(1 + K_o)}. \quad (11)$$

80 Extension-Cone

$$\sin \phi \geq \frac{3(1 - K_o)}{(1 + 5K_o)}. \quad (12)$$

81 Compromise-Cone

$$\sin \phi \geq \frac{3(1 - K_o)}{2(1 + 2K_o)}. \quad (13)$$

82 Internal-Cone

$$\sin \phi \geq \frac{(1 - K_o)}{\sqrt{K_o(2 + K_o)}}. \quad (14)$$

83 Fig. 4 presents the minimum ϕ values required to ensure elastic behavior under static conditions given
 84 by Eqs. (11) to (14). It is readily seen that the Compressional-Cone, yields real values of ϕ throughout the
 85 whole physical range of K_o (0 to 1). On the other hand, only a limited range of real values of ϕ is obtained
 86 from the rest of the cones. For instance, the Internal and Extensional cones only ensure elastic behavior for
 87 $K_o \geq 0.25$, while a relatively larger range is exhibited by the Compromise-Cone i.e. $K_o \geq 1/7 \approx 0.14$.

88 Using the K_o value predicted by Eq. (1), Eqs. (11) to (14) can be rewritten in terms of ν as:

89 Compression-Cone

$$\sin \phi \geq 1 - 2\nu. \quad (15)$$

90 Extension-Cone

$$\sin \phi \geq \frac{3(1 - 2\nu)}{(1 + 4\nu)}. \quad (16)$$

91 Compromise-Cone

$$\sin \phi \geq \frac{3(1 - 2\nu)}{2(1 + \nu)}. \quad (17)$$

92 Internal-Cone

$$\sin \phi \geq \frac{(1 - 2\nu)}{\sqrt{\nu(2 - \nu)}}. \quad (18)$$

93 Eqs. (15) to (18) are presented graphically in Fig 5. The Compression-Cone is the only stable approach

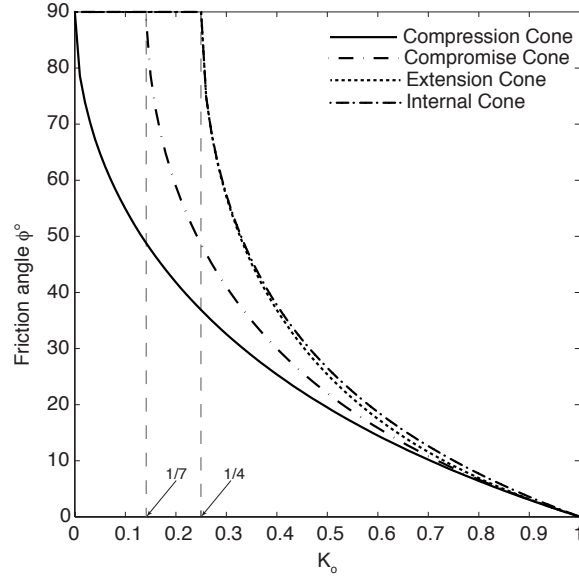


Figure 4: Minimum frictional angle ϕ required to ensure elastic behavior in terms of K_0 . Vertical dotted lines show the limiting values of (12) to (14).

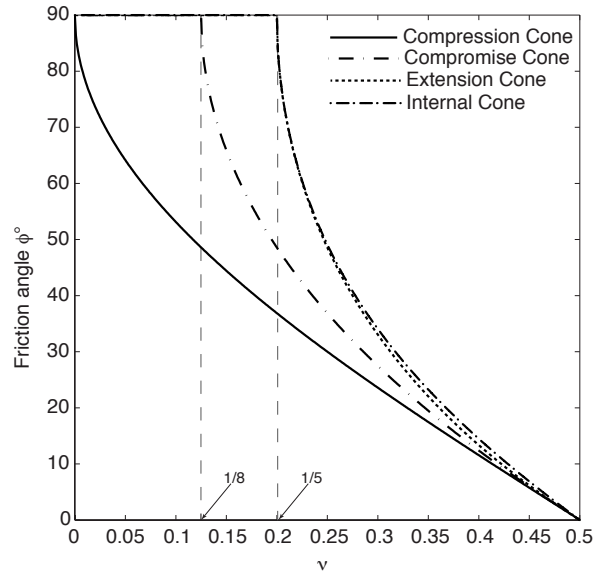


Figure 5: Minimum frictional angle ϕ required to ensure elastic behavior in terms of ν . Vertical dotted lines show the limiting values of (16) to (18).

94 that guarantees elastic behavior at rest conditions for the whole physical range of ν . This stable behavior,
 95 however, needs to be understood merely in the mathematical sense i.e. there is a real ϕ , for a real ν . From
 96 the physical point of view, some peculiar behavior can still emerge. For instance, rewriting Eq. (15) in
 97 terms of ν , one obtains the minimum Poisson's ratio that a half-space must hold in order to guarantee elastic

98 behavior under gravity forces for a fixed ϕ .

$$\nu \geq \frac{(1 - \sin \phi)}{2} . \quad (19)$$

99 Assuming for the sake of comparison a traditional value of $\phi = 30^\circ$, Eq. (19) shows that elastic behavior
100 is preserved only if $\nu \geq 0.25$. For lower values of ν , plastic behavior occurs irrespective of the matching
101 criterion with the Mohr-Coulomb model employed by the Drucker-Prager plastic surface.

102 The unusual plastic behavior predicted under static conditions raises doubts regarding the validity of
103 using these results as initial stress conditions in subsequent nonlinear analysis. This is specially true since
104 it is reasonable to expect that under the effects of just gravity the the level of strains in the mass of soil is
105 so small that linear behavior should prevail. Elastic behavior can be however restored by means of a *hybrid*
106 approach. This assumes that the functional form of the stress-state predicted from elastic theory is preserved,
107 see (Fig. 1), but modifies K_o by the widely used coefficient of lateral pressure at rest for consolidated clays
108 and granular-soils proposed by [Jaky \(1944\)](#):

$$K_o = 1 - \sin \phi , \quad (20)$$

109 with this in mind, the inequality in Eq. (11) yields:

$$\sin \phi \leq 1 . \quad (21)$$

110 It is readily seen that the latter is always satisfied for any ϕ . In contrast, the inequalities in Eqs. (12), (13),
111 and (14) turn into:

$$\sin \phi \leq 3/5 , \quad (22)$$

$$\sin \phi \leq 3/4 , \quad (23)$$

112 and

$$\sin \phi \leq (5 - \sqrt{13})/2 , \quad (24)$$

113 which are only satisfied by $\phi \leq 36.9^\circ$, $\phi \leq 48.5^\circ$, and $\phi \leq 44.2^\circ$ respectively. It is worth to notice that
114 despite the apparent limits of applicability of the latter values, these cover most of the range of friction angle

115 values of engineering interest.

116 **2 Conclusions**

117 The stress state from gravity loads predicted from elastic theory in a homogeneous half-space was examined
118 according to a cohesionless Drucker-Prager failure criterion. Analytical results showed that for a fixed
119 ϕ value, elastic behavior under gravity forces is ensured only for a particular range of Poisson's values,
120 i.e. $\nu \geq (1 - \sin \phi) / 2$. This irregular plastic behavior appears to challenge the widely accepted idea
121 of linear behavior under static conditions. It was shown however, that when the traditional coefficient
122 of lateral pressure for granular-soils is adopted, elastic condition at rest is recovered for any ϕ value for
123 the Compression Drucker-Prager cone. The rest of the approaches present limits of applicability in their ϕ
124 values, although those limits appear to cover the maximum limit of friction angles usually found in granular-
125 soils.

126 The previous results suggest that using elastic theory to assess the initial stress state from gravity loads
127 in general domains, can lead to an unrealistic nonlinear behavior at rest conditions in geomaterials with zero
128 or very low cohesion values. Fortunately, the fact that even for heterogeneous domains the self-weight value
129 γ is almost constant, the computation of the stress-state at rest can still be performed by means of the hybrid
130 approach followed in this study.

References

- 131
- 132 Borja, R. I. and Lee, S. R. (1990). Cam-clay plasticity, part 1: Implicit integration of elasto-plastic consti-
133 tutive relations. *Computer Methods in Applied Mechanics and Engineering*, 78(1):49 – 72.
- 134 Chen, W.-F. and Mizuno, E. (1990). *Nonlinear analysis in soil mechanics: theory and implementation*.
135 Amsterdam: Elsevier.
- 136 Daddazio, R., Ettouney, M., and Sandler, I. (1987). Nonlinear dynamic slope stability analysis. *Journal of*
137 *Geotechnical Engineering*, 113(4):285–298.
- 138 de Souza Neto, E. A., Perić, D., and Owen, D. R. J. (2008). *The mathematical Theory of Plasticity, in*
139 *Computational Methods for Plasticity: Theory and Applications*, chapter 6, pages 137–190. John Wiley
140 & Sons, Ltd.
- 141 Drucker, D. (1959). Definition of a stable inelastic material. *Journal of Applied Mechanics*, 26:101.
- 142 Drucker, D. C. and Prager, W. (1952). Soil mechanics and plastic analysis or limit design. *Quarterly of*
143 *Applied Mathematics*, 10:157–164.
- 144 Griffiths, D. (1990). Failure criteria interpretation based on mohr-coulomb friction. *J Geotech Engrg*,
145 116(6):986–999.
- 146 Jaky, J. (1944). The coefficient of earth pressure at rest. *Journal for the Society of Hungarian Architects*
147 *and Engineers*, October:355–358.
- 148 Ma, S. and Andrews, D. J. (2010). Inelastic off-fault response and three-dimensional dynamics of earthquake
149 rupture on a strike-slip fault. *Journal of Geophysical Research*, 115(B4).
- 150 Mizuno, E. and Chen, W. (1984). Plasticity models for seismic analyses of slopes. *International Journal of*
151 *Soil Dynamics and Earthquake Engineering*, 3(1):2 – 7.
- 152 Mizuno, E. and Chen, W.-F. (1983). Plasticity analysis of slope with different flow rules. *Computers &*
153 *Structures*, 17(3):375–388.
- 154 Restrepo, D., Karaoglu, H., Taborda, R., and Bielak, J. (2012). Implementation and application of inelastic
155 soil models in full 3d earthquake simulations. Technical report, Final Technical Report USGS Award
156 G11AP20127.

- 157 Templeton, E. L. and Rice, J. R. (2008). Off-fault plasticity and earthquake rupture dynamics: 1. dry
158 materials or neglect of fluid pressure changes. *Journal of Geophysical Research*, 113(B9).
- 159 Viesca, R. C., Templeton, E. L., and Rice, J. R. (2008). Off-fault plasticity and earthquake rupture dynamics:
160 2. effects of fluid saturation. *Journal of Geophysical Research*, 113(B9).
- 161 Zienkiewicz, O. and Pande, G. (1977). *Some Useful Forms of Isotropic Yield Surfaces for Soil and Rock*
162 *Mechanics, in Finite Elements in Geomechanics.*, pages 179–190. John Wiley and Sons.